Mean surface topography of the northwest Atlantic: Comparison of estimates based on satellite, terrestrial gravity, and oceanographic observations

K. R. Thompson,[1] J. Huang,[2] M. Véronneau,[2] D. G. Wright,[3] and Y. Lu[4]

Received 10 April 2008; revised 16 January 2009; accepted 24 March 2009; published 15 July 2009.

[1] The accuracy of a new mean sea surface topography (MSST) of the northwest Atlantic is assessed. The MSST is estimated from 12 years of altimeter observations referenced with respect to a new regional geoid based on a blend of Gravity Recovery and Climate Experiment (GRACE), terrestrial, and altimeter-derived gravity data. The new MSST is first compared to a recently published mean surface topography calculated using an eddy-permitting model of the North Atlantic. Geostropic currents calculated from the GRACE-based MSST are next compared to mean surface currents in the northwest Atlantic estimated from the motion of near-surface drifters corrected for surface Ekman effects. Finally, the mean path of the Gulf Stream is compared to the line of zero skewness of sea level variability which provides a measure of the mean path of unstable, intense ocean currents. Overall the agreement amongst the various estimates of surface topography and circulation is excellent. There are, however, some significant differences that can be separately attributed to problems with the MSST and, in some cases, with the ocean model (in particular the ocean climatology to which it was nudged).

Citation: Thompson, K. R., J. Huang, M. Véronneau, D. G. Wright, and Y. Lu (2009), Mean surface topography of the northwest Atlantic: Comparison of estimates based on satellite, terrestrial gravity, and oceanographic observations, *J. Geophys. Res.*, *114*, C07015, doi:10.1029/2008JC004859.

1. Introduction

[2] The altimeter is arguably the most important spaceborne sensor for physical oceanographic applications. It has been used extensively for over two decades to map mesoscale variability of the World Ocean [e.g., *Ducet and Le Traon*, 2001] and, more recently, it has become a critical data stream for assimilation into operational forecast models [e.g., *Le Traon*, 2002].

[3] Altimeters can measure mean sea surface height (MSSH) relative to a reference ellipsoid with an accuracy of about 4 cm between 66°N to 66°S. To estimate mean surface currents it is necessary to find the mean sea surface topography (MSST) which is the height of sea level with respect to its undisturbed level, i.e., MSST = MSSH - N where N is the height of the geoid, defined with respect to the same reference ellipsoid as the MSSH. Unfortunately, the geoid has not been defined with sufficient accuracy to allow the calculation of useful absolute surface currents from altimeters [e.g., *Tapley et al.*, 2003].

[4] The Gravity Recovery and Climate Experiment (GRACE) satellite mission [e.g., *Tapley et al.*, 2004; *Reigber et al.*, 2005] is a recent attempt to improve the specification of the geoid and its time variation. Two satellites in identical orbits, separated by about 200 km, were launched on 17 March 2002. By measuring the distance between the two satellites it has been possible to map the gravity field, and its time dependence, with unprecedented accuracy and resolution. Initial indications are that this mission has improved the determination of the gravity field by at least a factor of 10 over all previous satellite missions, leading to a geoid accuracy of about 2 cm on scales longer than about 400 km [e.g., *Tapley et al.*, 2004]. The GRACE data is also providing valuable information on changes in the Earth's mass distribution and this is leading to new insights about geodynamic processes such as glacial isostatic adjustment of the Earth's crust (R. Peltier, personal communication, 2008).

[5] Major ocean currents can vary significantly on scales of a few tens of kilometers. Unfortunately, it is at these relatively short spatial scales where the accuracy of the geoid is subject to the greatest uncertainty. One way to improve the accuracy of GRACE-based geoids at high wave number is to blend the GRACE gravity data with observations made from land, airborne and marine platforms. In this study we describe a new MSST for the northwest Atlantic

[1]Department of Oceanography, Dalhousie University, Halifax, Nova Scotia, Canada.
[2]Geodetic Survey Division, CCRS, Natural Resources Canada, Ottawa, Ontario, Canada.
[3]Department of Fisheries and Oceans, Bedford Institute of Oceanography, Dartmouth, Nova Scotia, Canada.
[4]Environment Canada, Dartmouth, Nova Scotia, Canada.

0148-0227/09/2008JC004859

based on altimeter measurements of MSSH and a regional geoid obtained by blending GRACE, terrestrial and altimeter-derived gravity observations. We will henceforth refer to this new mean sea surface topography as $MSST_{G1}$. The main purpose of this study is to assess the realism of $MSST_{G1}$ using independent information on the surface topography, and the surface circulation, of the northwest Atlantic. This study focuses on water depths greater than 200 m. This effectively removes the tidally dominated, and occasionally ice covered, continental shelves from the analysis where the altimetric data is subject to relatively large errors and seasonal biases. To determine the contribution of the terrestrial gravity data, we also evaluate an MSST that was calculated without the terrestrial gravity data ($MSST_{G0}$).

[6] The first evaluation of $MSST_{G1}$ is based on results from an eddy-permitting model forced by realistic surface fluxes of heat, freshwater and momentum and spectrally nudged toward an observed climatology of temperature and salinity in the interior. We will henceforth refer to this new model-based topography as $MSST_M$. The details of the calculation, and a map of $MSST_M$, were published recently by *Thompson et al.* [2006].

[7] The second evaluation of $MSST_{G1}$ is based on near surface velocities derived from the motion of drifting buoys [*Niiler*, 2001]. After correction for the wind-driven Ekman flow, the drifter velocities can be interpreted in terms of geostrophic flow and thus tilts of the sea surface. We compare the geostrophic currents from drifters with those calculated from the spatial gradients of $MSST_{G1}$, focusing on the Gulf Stream and Labrador Current.

[8] The final evaluation of $MSST_{G1}$ uses skewness of sea level variability measured by altimeters. *Thompson and Demirov* [2006] recently showed that skewness, and in particular the zero skewness contour, can be used as a measure of the mean position of variable ocean currents. Note that the skewness of sea surface height depends only on temporal variations of sea level and so this estimate of the mean path does not depend on the specification of the geoid. We use the zero contour line to assess the reliability of $MSST_{G1}$ in the Gulf Stream region.

[9] The main differences between the present study and earlier studies [e.g., *Bingham and Haines*, 2006; *Jayne*, 2006; *Rio and Hernandez*, 2004] are the use of (1) a new regional geoid, based on blending GRACE, terrestrial, and altimeter-derived gravity data, leading to a more accurate determination of the geoid at high wave numbers; (2) an oceanographically determined MSST based on the assimilation of a new ocean climatology using the spectral nudging technique; and (3) sea level skewness to check the mean path of an unstable ocean current. Together with the drifter data these considerations allow a detailed assessment of the strengths and weaknesses of $MSST_{G1}$ and $MSST_M$, and the value of using terrestrial gravity data.

[10] The structure of the paper is as follows. In section 2, the calculation and structure of $MSST_{G0}$ and $MSST_{G1}$ are described and in section 3 they are compared to the mean surface topography of the ocean model, $MSST_M$. In section 4 geostrophic currents based on drifter data are compared with surface geostrophic currents calculated from gradients of $MSST_{G0}$, $MSST_{G1}$ and $MSST_M$. Sea level skewness is discussed in section 5 and used to further assess the reliability of the mean sea surface topographies. The implications of the generally good agreement, and prospects for future work, are discussed in the final section.

2. MSST Based on Altimeter and Gravity Data

[11] This section outlines the calculation of a new regional geoid for the northwest Atlantic. The geoid is then subtracted from direct satellite measurements of sea surface height to give a new, geodetically determined mean sea surface topography.

2.1. Mean Sea Surface Height

[12] The surface height field used in this study is the GSFC00 global model of *Wang* [2001]. It is based on 6 years of TOPEX data, 1.5 years of ERS-1 track data, 3 years of ERS-2 data, and 2 years of Geosat data. The data were collected between 1986 and 1999. The spatio-temporal means of the non-TOPEX data were adjusted to the corresponding 6-year mean of the TOPEX data. Note that this adjusts the overall mean sea level, but not the mean sea level gradients that are related to the surface geostrophic flow. The standard error of the mean sea surface height field is largest (order 8 cm) on continental shelves, presumably the result of high-frequency variability due to tides and atmospheric forcing, and varying ice cover. Another region with relatively large standard errors is the Gulf Stream region where the standard deviation of instantaneous sea level can reach almost 50 cm in some locations. In the Gulf Stream region, the standard error of the mean sea surface height field is 5 to 6 cm; over the rest of the North Atlantic the standard error is about 3 cm.

2.2. Geoid Height

[13] A new regional geoid for the North Atlantic (7°N to 67°N, 99°W to 20°E) has been calculated by blending GRACE, terrestrial and altimeter-derived gravity data using the Stokes-Helmert method [*Heiskanen and Moritz*, 1967; *Vanìcek and Martinec*, 1994; *Huang and Véronneau*, 2005]. The GRACE data is used to define the geoid at low wavelengths and the terrestrial and altimeter-derived gravity data define the geoid at high wave numbers. The resolution of the geoid is a function of the density of the gravity observations (see Appendix A for details.) The GGM02C model of *Tapley et al.* [2005] was used to define the GRACE-based gravity and geoid values using spherical harmonics ranging from degree 2 to 60 (corresponding to a nominal horizontal resolution of 10,000 km and 330 km, respectively). The terrestrial gravity data set includes land observations from Canada and the United States, shipboard observations from the east coast of Canada (extending seaward about 500 km; see Figure 1), and airborne data from Greenland. Ocean areas without terrestrial gravity measurements were filled with altimetry-derived gravity data. (Note that new ArcGP gravity and ice thickness data, and an improved digital terrain model, have recently become available for Greenland. This may improve to some degree the geoid offshore of Greenland. Because of the large amount of work involved in recomputing the geoid in this region, consideration of these new data will be reserved for future studies.)

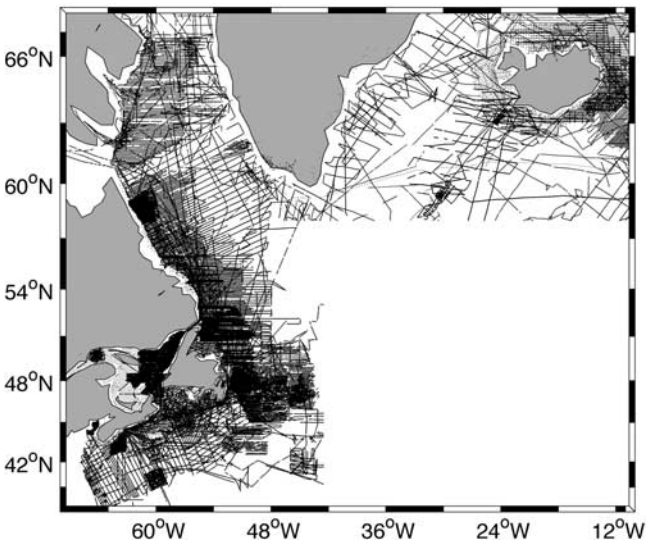

Figure 1. Locations of the shipboard gravity observations. These observations were combined with land observations from Canada and the United States and airborne observations from Greenland in the calculation of the geoid for $MSST_{G1}$.

[14] The new regional geoid was calculated on a grid with a spacing of 1/30°. Both the geoid and the MSSH were defined in the mean tide system. On the basis of a formal error analysis (Appendix A) we conclude that the standard error of the regional geoid is about 3 cm within about 500 km of the east coast of Canada. Outside of this region the standard error is estimated to be about 6 cm. More details on the new geoid and its calculation are given in Appendix A.

2.3. Mean Sea Surface Topography

[15] The mean sea surface topography was obtained by subtracting the new regional geoid from the mean sea surface height described above. The standard error of the sea surface topography, based on the standard errors of geoid and sea surface height, are generally less than 8 cm over most of the North Atlantic, and about half this value within about 500 km of the east coast of Canada where the terrestrial gravity data have been used.

[16] To compare the new topography to results from the ocean model and the drifter data, the 1/30° values were mapped to a grid with a spacing of 1/3° in longitude and a latitudinal spacing that decreases with latitude such that grid boxes remain approximately square. The mapping was carried out using the median of all 1/30° values within ±1/6° of each grid point. The resulting topography ($MSST_{G1}$, Figure 2) is consistent with overall oceanographic expectations. The subpolar and subtropical gyres and their western boundary currents, including the Gulf Stream after it leaves the coast at Cape Hatteras, are clearly evident. The Mann Eddy [*Mann*, 1967] can also be seen at about 44°W, 42°N. Further south one can see the generally northward flow through the Caribbean into the Gulf of Mexico, the Loop Current, and the flow through the Florida Strait. There are however some unrealistic features including high wave number variability to the south of Iceland and spikes in the vicinity of Madeira, the Canary Islands and Cape Verde. These features coincide with sectors where the shipboard gravity tracks are sparse and inaccurate (Iceland) and where the accuracy of the satellite-derived gravity was not validated (islands off the west coast of Africa) because they fell outside the scope of the geoid modeling for Canada and its adjacent waters. The small wiggles of the isolines evident in Figure 2 are caused by short-wavelength inaccuracies in the GSFC00 sea surface height model.

[17] To quantify the sea level contribution from the terrestrial gravity data, we generated a spherical harmonic model of MSSH by combining the GSFC00 MSSH model over the oceans and the GGM02S geoid model over land. We then subtracted the GGM02S geoid model to create $MSST_{G0}$. The full set of spherical harmonics of GGM02S up to degree 60 were used; from degree 60 to 90 the amplitude of the harmonics decreased smoothly to zero (similar to the blended solution, see Appendix A). As expected, the new topography ($MSST_{G0}$, Figure 3) is smoother than $MSST_{G1}$ with the largest differences occurring in the regions where terrestrial gravity data were used (Figure 4). In the vicinity of the Gulf Stream and Labrador Current the terrestrial and altimeter-derived gravity causes spatially coherent changes of about 10 cm and 20 cm, respectively; for both regions the addition of terrestrial and altimetry-derived gravity data tends to increase the strength of local boundary currents.

3. MSST From an Ocean Model

[18] *Thompson et al.* [2006] recently calculated the MSST of the North Atlantic using a z-coordinate, hydrostatic, general ocean circulation model with an implicit free surface. Relevant model details are given in Appendix B. To suppress drift and bias, the model's temperature and salinity

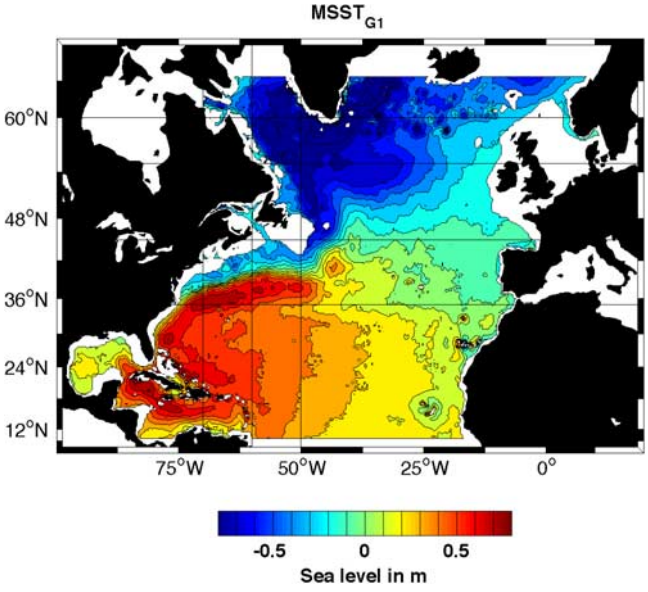

Figure 2. Mean sea surface topography based on GRACE, terrestrial, and altimetry-derived gravity data ($MSST_{G1}$). Areas shallower than 200 m, the Pacific and Mediterranean, and the model's sponge layers were excluded, following which the spatial mean was removed. The black lines define the sections plotted in Figure 6.

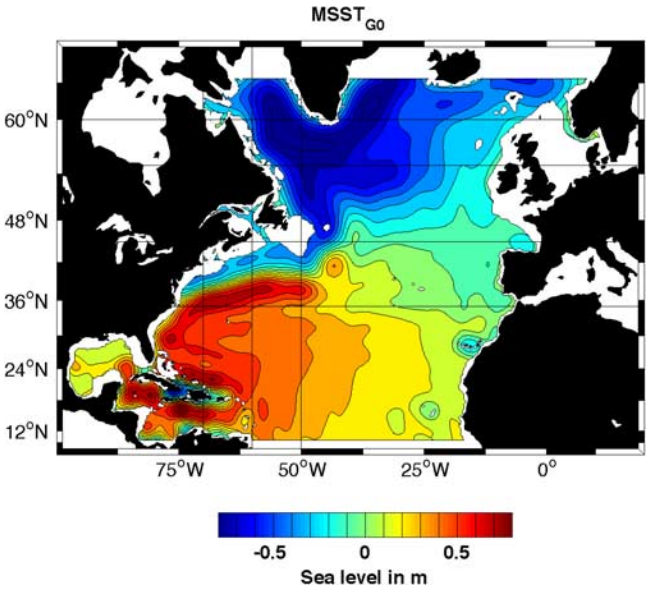

Figure 3. Mean sea surface topography based on only GRACE gravity data ($MSST_{G0}$). Format is the same as Figure 2.

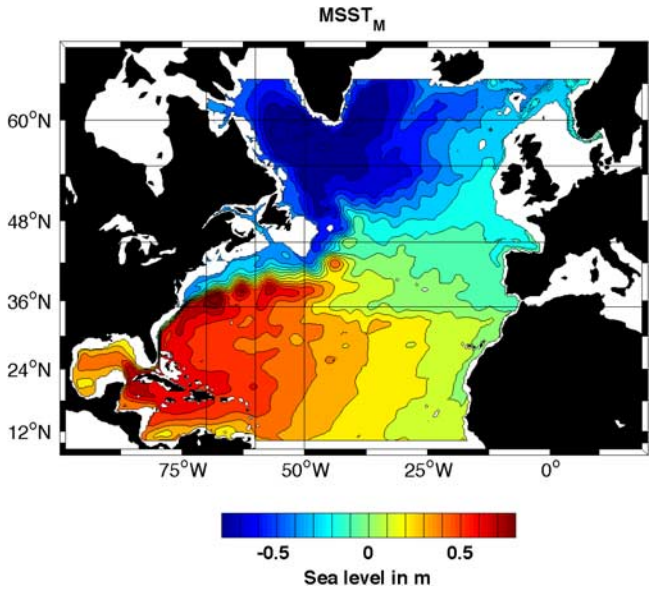

Figure 5. Mean sea surface topography based on output from the ocean model ($MSST_M$) (see *Thompson et al.* [2006] and text for details). Format is the same as Figure 2.

fields were restored to the seasonal climatology of Yashayaev (see www.mar.dfo-mpo.gc.ca/science/ocean/woce/climatology/naclimatology.htm) using ''spectral nudging.'' The basic idea is to nudge the model in selected frequency and wave number bands; outside these bands the model is free to evolve ''prognostically.'' The nudged frequency bands are centered on the climatological frequencies of 0 and 1 cycle per year and the nudged wavelengths are a few hundred km or longer (for details see *Thompson et al.* [2006]). This type of calculation is more sophisticated than a simple dynamic height calculation based on an assumed level of no motion, or a diagnostic calculation with prescribed density field; it is closer in spirit to a robust diagnostic calculation [*Sarmiento and Bryan*, 1982]. A discussion and comparison of such methods is given by *Thompson et al.* [2006]. More details on the implementation of spectral nudging are given in Appendix B.

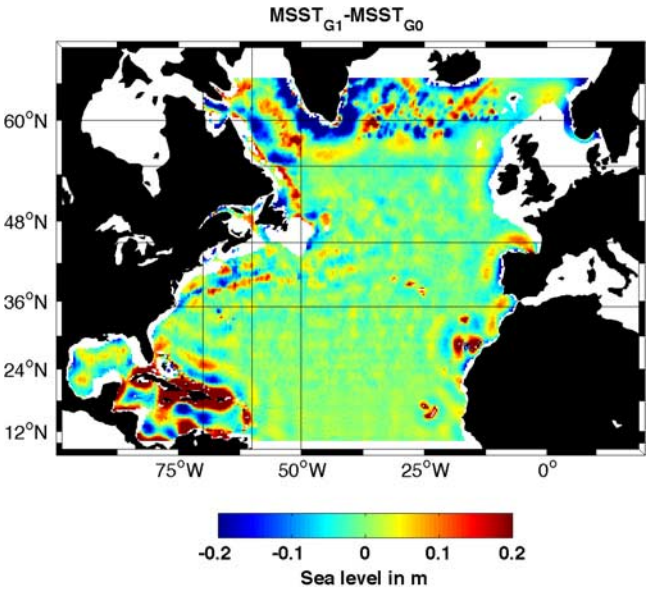

Figure 4. Difference of $MSST_{G1}$ and $MSST_{G0}$ showing the effect of the terrestrial and altimetry-derived gravity data. Format is the same as Figure 2 except for the colorbar.

[19] The ocean model's sea surface topography ($MSST_M$, Figure 5) is visually similar to $MSST_{G1}$ both in terms of its broad-scale structure and some of the details. In particular, the sea level variation associated with the subpolar and subtropical gyres, and the Mann Eddy, are similar in the two estimates of surface topography.

[20] A more quantitative comparison of the two topographies is given in Figure 6 which shows sea level along selected zonal and meridional sections. The agreement is encouraging, in terms of both the overall shape and the amplitude of the variations. The western boundary currents are clearly evident in the tilts of sea level including the Gulf Stream and offshore branch of the Labrador Current.

[21] The standard deviation of $MSST_{G1}$ shown in Figure 2 is 42 cm; the corresponding standard deviation of $MSST_{G1}$-$MSST_M$ is only 8 cm. The standard deviation of the difference is higher (11 cm; see Table 1) in the relatively energetic Gulf Stream region, but lower in the vicinity of the Labrador Current (6 cm; see Table 2). Another way of comparing the two topographies is with their correlation; they are 0.97 and 0.95 in the Gulf Stream and Labrador Current regions, respectively (see Tables 1 and 2). Overall the standard deviation of differences and correlations confirm the visual similarity of $MSST_{G1}$ and $MSST_M$ noted above.

[22] Although the correlation between $MSST_{G1}$ and $MSST_M$ is high, there are still some dynamically important differences that exceed 20 cm in the vicinity of the Gulf Stream and Labrador Current. For example, (1) the ocean

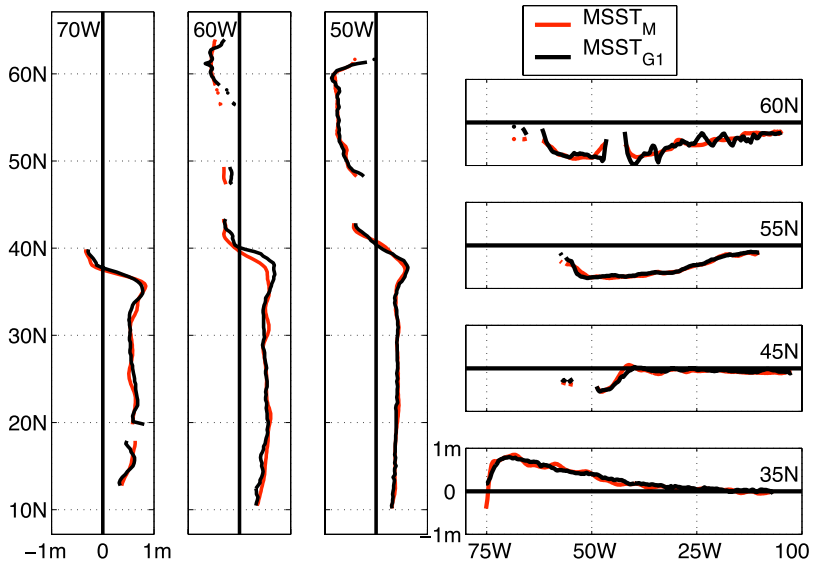

Figure 6. Zonal and meridional sections of mean sea surface topography based on the ocean model ($MSST_M$) and the GRACE, terrestrial, and altimeter-derived gravity-based geoid ($MSST_{G1}$). The sections are indicated in Figure 5.

model's Gulf Stream has large-scale meanders in its path that are not evident in $MSST_{G1}$ (compare Figures 2 and 5), (2) the Florida Current in $MSST_M$ is substantially faster than in $MSST_{G1}$ (compare the tilts of sea level in the 35N section of Figure 6), (3) the Labrador Current in $MSST_M$ is weaker and broader than $MSST_{G1}$ (compare the tilts of sea level in the 60°N section of Figure 6). To understand the reasons for these differences, $MSST_{G1}$ and $MSST_M$ are now compared to additional independent oceanographic data.

4. Surface Drifter Data

[23] The Global Drifter Program aims to maintain a global array of over 1000 surface drifting buoys that can provide in situ observations of surface currents, sea surface temperature, atmospheric pressure, winds and salinity of the world's oceans [e.g., *Niiler*, 2001]. In this section surface geostrophic velocities, estimated from the historical archive of drifter data, are compared with geostrophic velocities inferred from $MSST_M$, $MSST_{G0}$ and $MSST_{G1}$.

[24] The initial data set was provided by P. Niiler and contained the positions, velocities and times of a global distribution of drifters drogued at 15 m. (The processing of the data is described by *Niiler* [2001].) The drifter measurements for the North Atlantic were made between January 1980 and December 2005, but over 90% were made between August 1993 and December 2005. To estimate surface geostrophic velocities, the drifters' velocities were binned according to the ocean model grid (see above and Appendix B) and then corrected for surface Ekman flow using the method of *Niiler and Paduan* [1995].

4.1. Gulf Stream

[25] The Florida Current originates in the Gulf of Mexico and flows northward to Cape Hatteras. At this location the current turns seaward and continues eastward as an unstable, open ocean jet called the Gulf Stream. It is typically 100 km wide and attains speeds that can exceed 2 m s^{-1}. Meanders in the Gulf Stream are often observed to grow and eventually pinch off to form both warm and cold core rings. The Gulf Stream splits at the Tail of the Grand Bank to form several branches including the Azores Current and the North Atlantic Current (see *Reverdin et al.* [2003] for a review). The map of surface geostropic speed according to the drifters, shown in Figure 7a, is consistent with this description. The Gulf Stream can clearly be seen leaving the continental slope near Cape Hatteras with a peak mean speed that exceeds 1 m s^{-1}. It continues eastward as a narrow, decelerating jet with peak speeds that drop to about 0.4 m s^{-1} by 52°W.

[26] The map of surface geostropic speed inferred from $MSST_{G0}$ is shown in Figure 7c. The Gulf Stream can clearly

Table 1. Statistics of Fit in the Vicinity of the Gulf Stream[a]

	Y	P_0	P_1	$Y - P_0$	$Y - P_1$	ρ_{YP0}	ρ_{YP1}
η (cm)	20.4 (41.7)	23.4 (39.2)	23.2 (40.0)	(10.5)	(10.5)	0.97	0.97
u (cm s^{-1})	9.7 (22.0)	8.9 (15.6)	9.0 (18.1)	(16.1)	(15.9)	0.68	0.70
v (cm s^{-1})	2.9 (13.2)	1.8 (5.7)	1.9 (9.7)	(11.3)	(13.1)	0.53	0.39

[a]See Figure 7 for domain. Y refers to independent data used to check predictions, P_0 and P_1, on the basis of $MSST_{G0}$ and $MSST_{G1}$, respectively. The first five columns of numbers show the mean and standard deviation of the independent data, the predictions, and their differences. Standard deviations are shown in parentheses. The last two columns show the correlation between the independent data and the predictions. For sea level (η), Y refers to sea level predicted by the ocean model ($MSST_M$). For eastward (u) and northward (v) geostrophic flow, Y refers to the gridded drifter observations.

Table 2. Statistics of Fit in the Vicinity of the Labrador Current[a]

	Y	P_0	P_1	$Y - P_0$	$Y - P_1$	$\rho_{Y,P0}$	$\rho_{Y,P1}$
η (cm)	−59.8 (15.5)	−56.4 (17.4)	−57.9 (18.3)	(5.3)	(6.0)	0.95	0.95
u (cm s^{-1})	5.5 (14.1)	5.2 (6.1)	6.5 (13.5)	(11.7)	(10.1)	0.57	0.73
v (cm s^{-1})	0.1 (12.2)	−0.1 (3.9)	−0.3 (9.7)	(11.3)	(10.5)	0.39	0.56

[a]See Figure 9 for domain. The format is the same as Table 1 except that u and v refer to current components positive to the southeast and northeast, respectively.

be identified but it is too broad and its peak speeds are too low (less than 0.5 m s^{-1}), consistent with the study of *Jayne* [2006]. The effect of adding the terrestrial and altimetry-derived gravity data can be seen in Figure 7d which shows the surface geostropic speed inferred from $MSST_{G1}$. There is now much better agreement with the drifter map in terms of the width of the Gulf Stream, its path and peak speeds.

[27] The means and standard deviations of the geostrophic velocities shown in Figure 7, and their differences, are given in Table 1. Although $MSST_{G1}$ would appear visually to give a better prediction of the drifter velocities than $MSST_{G0}$ this is not reflected in the standard deviation of the differences of eastward flow. (The standard deviations of the u error for $MSST_{G0}$ and $MSST_{G1}$ are both 16 cm s^{-1}.) To explain this discrepancy, consider a predicted velocity field that is perfect apart from a small horizontal displacement error. If the displacement is large in comparison to the dominant length scales of variability, the standard deviation of the differences of colocated observations and predictions will exceed the standard deviation of the observations. In such a situation one can expect that spatial smoothing of the prediction (and thus the loss of true detail) will improve the fit.

[28] To allow for the possibility that the error statistics given in Table 1 are influenced by small latitudinal errors in the position of the Gulf Stream we have plotted, in Figure 8, the peak speed of the Gulf Stream as a function of longitude. This approach gives results that are insensitive to the latitudinal position of the Gulf Stream. It is clear from Figure 8 that $MSST_{G0}$ has underestimated the speed of the Gulf Stream and that the use of terrestrial and altimetry-derived gravity data has improved significantly the realism of the geoid, and thus the MSST, east of about 67°W. It is interesting to note that both $MSST_{G0}$ and $MSST_{G1}$ underestimate significantly the speed of the Gulf Stream close to the separation point at Cape Hatteras. We speculate the reason is that terrestrial gravity data from the United States, west of about 67°W, were not used (see Figure 1) and thus the geoid may not be as well defined in this region compared to further east.

4.2. Labrador Current

[29] The Labrador Current is a relatively cold and fresh western boundary current that flows along the continental shelf and slope from Hudson Strait (60°N) to the Tail of the Grand Bank (43°N). Most of the flow is concentrated in a

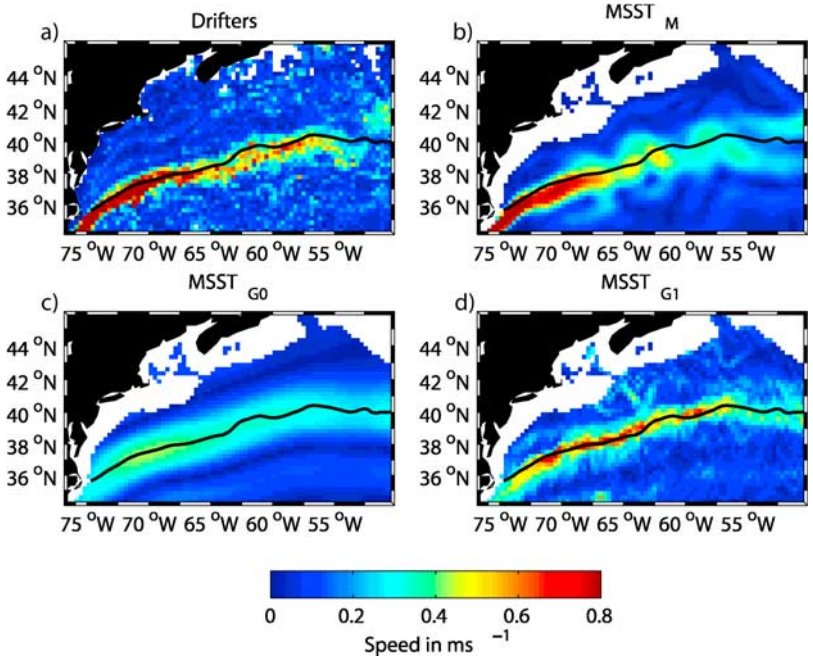

Figure 7. Surface geostrophic speed and the contour of zero sea level skewness in the vicinity of the Gulf Stream. (a) The speed of the binned drifter observations (after removal of the Ekman effect as explained in the text). (b) Geostrophic speed calculated from the surface topography from the ocean model. (c, d) Geostrophic speeds calculated from $MSST_{G0}$ and $MSST_{G1}$. The black line is the contour of zero sea level skewness (see Figure 10).

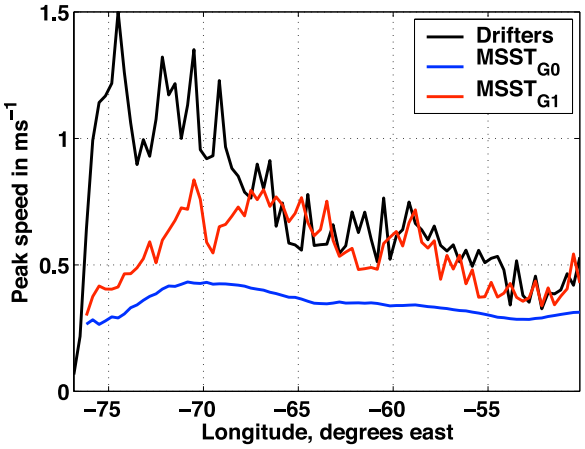

Figure 8. Peak speed of the Gulf Stream as a function of longitude. The peak speeds were calculated as a function of longitude from the speed maps shown in Figure 7. The difference between the red and blue lines is due to use of terrestrial and altimeter-derived gravity data to define the geoid.

narrow (approximately 50 km) current that flows along the upper continental slope with mean speeds between about 0.3 and 0.5 m s^{-1}. The path of the Labrador Current is strongly controlled by bathymetry and onshore branches have been observed to flow between the main banks on the outer shelf. For a detailed review of the Labrador Current see *Lazier and Wright* [1993].

[30] The map of geostrophic speed based on drifter data (Figure 9a) is generally consistent with the above description of the Labrador Current. The Labrador Current is clearly detectable, flowing between the 300 and 1000 m depth contours from 57°N to 55°N after which it flows around the seaward edge of Hamilton Bank at about 54°N. There is evidence in the speed plot for onshore flow between Hamilton and Belle Isle Bank at about 53°N. The Labrador Current is detectable to about 51°N. It can be detected again as an intense jet at about 49°N as it starts to flow around the edge of the Grand Banks with speeds of 40 to 50 cm s^{-1}. There is evidence for a bifurcation of the flow at about 48°N as some of the Labrador Current passes around the seaward edge of Flemish Cap.

[31] The map of surface geostropic speed calculated from MSST$_{G1}$ exhibits many of the features evident in the plot of drifter speed (compare Figures 9a and 9d). For example, the Labrador Current can be detected along the shelf slope and there is some evidence for onshore flow between Hamilton and Belle Isle Bank (at about 54°N), and between Belle Isle and Funk Island Bank (at about 52.5°N). The MSST$_{G1}$ also predicts a bifurcation in the Labrador Current as it flows around Flemish Cap, consistent with the drifter observations.

[32] The similarity of the velocities calculated from the drifters and MSST$_{G1}$ is quantified in Table 2. According to the drifters, the mean and standard deviation of the flow to the southeast are 6 cm s^{-1} and 14 cm s^{-1}, respectively. The corresponding values for MSST$_{G1}$ are 7 cm s^{-1} and 14 cm s^{-1}. Of more interest is the standard deviation of the difference in observed and predicted currents, and their correlation; for the dominant southeastward component of flow they are 10 cm s^{-1} and 0.73, respectively. The reduced standard deviation and high correlation are consistent with the visual similarity evident in Figure 9.

[33] The Labrador Current calculated from MSST$_{G0}$ is too weak and too wide (compare Figures 9a and 9c). The standard deviation of the differences of the observed and predicted flow components, and their correlation (Table 2), also show that the currents calculated from MSST$_{G0}$ do not agree with the drifters as well as the currents from MSST$_{G1}$.

5. Sea Level Skewness

[34] *Thompson and Demirov* [2006] recently examined the relationship between sea level skewness, which is calculated independently of the local mean sea level, and the mean path of major current systems of the world's oceans. It was shown that the line of zero skewness coincides with the mean path of unstable currents like the Gulf Stream (as defined, for example, by the maximum current speed or, equivalently, the maximum sea level gradient). Here, we compare the mean Gulf Stream path estimated from the skewness of sea level with the geo-

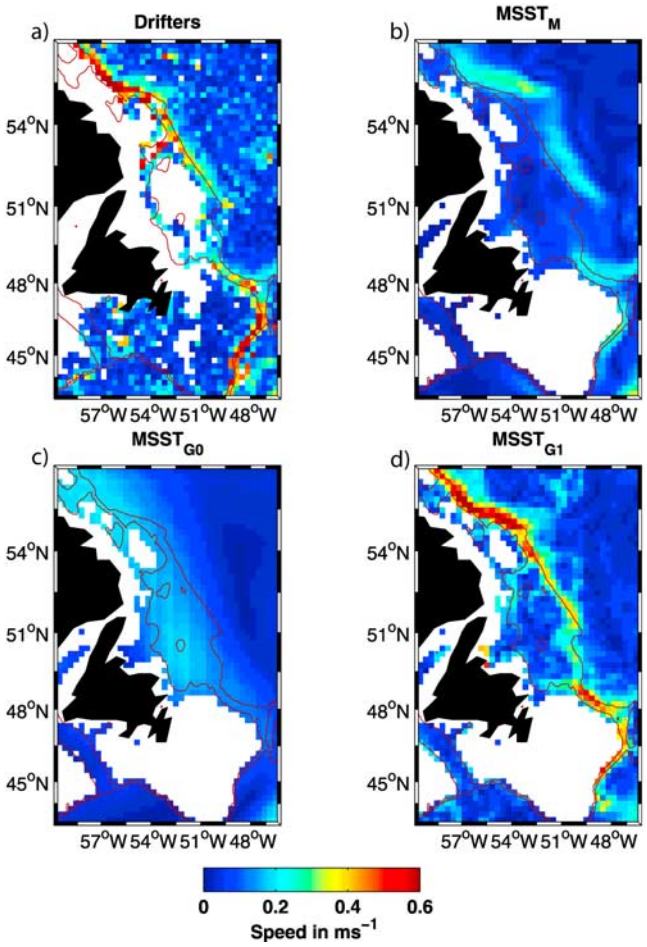

Figure 9. Surface geostrophic speed in the vicinity of the Labrador Current. The format is the same as Figure 7 except that the zero skewness line has been replaced by the 300 m and 1000 m depth contours.

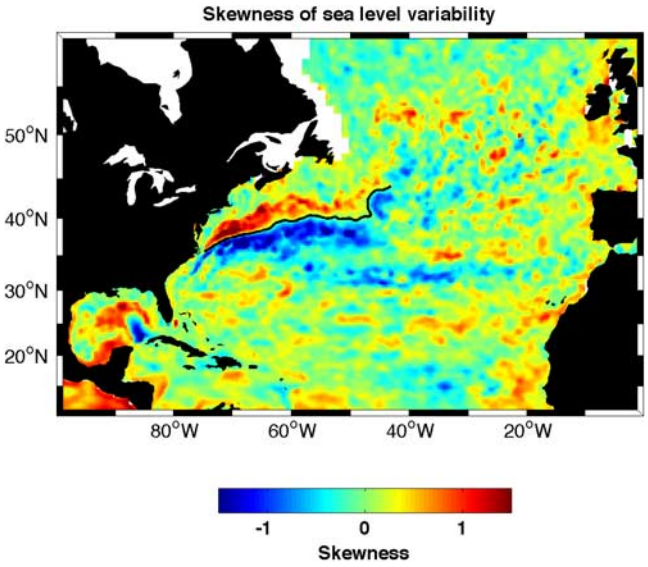

Figure 10. Skewness of sea level variability determined from altimeter observations. See *Thompson and Demirov* [2006] for details. The zero skewness contour line in the strong gradient region in the northwest Atlantic is also shown.

strophic current estimates presented in Figure 7. (We do not perform a similar analysis for the Labrador Current because its path is strongly controlled by bathymetry and so sea level skewness is not useful.)

[35] A map of skewness for the North Atlantic, calculated by *Thompson and Demirov* [2006] from gridded altimeter data, is shown in Figure 10. The solid black curve in Figure 10 corresponds to the zero line in skewness over the range where it can be unambiguously determined. According to the reasoning presented by *Thompson and Demirov* [2006] this zero line should coincide with the mean path of the Gulf Steam.

[36] The zero skewness line shown in Figure 10 has been added to the speed plots shown in Figure 7. Away from the continental slope, the zero skewness line tracks the path of maximum current speed quite closely for the drifters and $MSST_{G1}$. This is encouraging in that it provides another validation of the flow field, sea surface topography, and thus geoid, associated with $MSST_{G1}$.

[37] There is a tendency for the maximum drifter speeds to be slightly south of the zero skewness line in the vicinity of Cape Hatteras by about 30 km. The reasons for this are not clear at this point but they may be related to the difference in the period of altimeter data (1993 to 2001) and drifter data (90% between 1993 and 2005). Another possibility is that the latitudinal displacements of the Gulf Stream may also be skewed, i.e., near the continental slope, the stream may at times shift offshore, but it cannot shift significantly onshore. More work is required to test these speculations.

[38] The geostrophic speeds calculated by the ocean model are also displaced slightly south of the zero skewness line west of about 67°W (Figure 7b). There are also differences in the skewness line and the path of the Gulf Stream predicted by the model east of 67°W. In particular the model predicts large oscillations in the path that are not seen in the zero skewness line or the drifter speeds. The explanation may be that $MSST_M$ is strongly controlled by the climatology to which it is spectrally nudged. The hydrographic data used to form the climatology were collected over much of the last century and it is possible the climatology may have aliased the pronounced low-frequency variability that is known to occur in this energetic region [e.g., *Hakkinen and Rhines*, 2007]. In other words, the zero skewness line, the drifter data and $MSST_{G1}$ may be pointing to problems with the climatology to which the model was nudged. Support for this speculation comes from some recent sensitivity studies (not presented here) in which increased spatial smoothing of the nudges in the ocean model reduce significantly the meandering of the mean Gulf Stream.

6. Discussion

[39] The primary purpose of the present study is to evaluate a new mean sea surface topography of the northwest Atlantic that is based on a blend of GRACE, terrestrial and altimetry-derived gravity data. The overall conclusion is that the new topography ($MSST_{G1}$) is in good agreement with independent estimates of the mean sea surface topography from an ocean model ($MSST_M$) and surface circulation features inferred from observed drifter trajectories and the skewness of observed sea level variability. Many well known circulation features in the northwest Atlantic, where most of the terrestrial gravity data were collected, are clearly evident in $MSST_{G1}$ including the Gulf Stream, the Mann Eddy, the Labrador Current and the westward flow around the southern tip of Greenland. It is encouraging to note that $MSST_{G1}$ resolves oceanographic features with length scales of order 100 km (e.g., the Mann Eddy, which has a radius of about 50 km, and the Gulf Stream which is about 100 km wide).

[40] The terrestrial and altimeter-derived gravity data were used to add high wave number detail to the marine geoid and thus to $MSST_{G1}$ in the northwest Atlantic. To assess the realism of this detail, we also evaluated a surface topography ($MSST_{G0}$) that was calculated without the use of terrestrial and altimeter-derived gravity data. It was shown that many oceanographic features were too weak and diffuse in $MSST_{G0}$. For example, the peak speeds in the Gulf Stream at 67°W are about 0.7 m s^{-1} according to the drifters and $MSST_{G1}$ but only 0.4 m s^{-1} according to $MSST_{G0}$. Another example is found in the standard deviation of the southeast flow in the vicinity of the Labrador Current; it is about 14 cm s^{-1} according to the drifters and $MSST_{G1}$ but only 6 cm s^{-1} according to $MSST_{G0}$. The superior fit of $MSST_{G1}$ to independent oceanographic data clearly demonstrates the valuable information added by the additional gravity data at higher wave numbers. An obvious extension of the present study would be to include more terrestrial data near Cape Hatteras to better resolve the Gulf Stream west of 67°W and also other oceanographically interesting regions with large sea level signals (e.g., Caribbean and southern tip of Greenland).

[41] One of the novel aspects of the present evaluation of sea surface topographies is the use of sea level skewness.

It was shown that the zero skewness line coincides closely with the mean path of the Gulf Stream inferred from $MSST_{G1}$ and the drifter data. We anticipate that the zero skewness contour may prove useful in evaluating mean sea surface topographies for other regions, particularly those with lower densities of drifter observations than the Gulf Stream region. Note that the skewness was not useful in the Labrador Current region because the path of this current is strongly constrained by the bathymetry.

[42] The standard deviation of $MSST_{G1}$ across the North Atlantic is 42 cm; the corresponding standard deviation of $MSST_{G1}$-$MSST_M$ is only 8 cm. Thus most of the spatial variability in $MSST_{G1}$ can be explained by the ocean model. There are however differences that exceed 30 cm in some regions, including the Gulf Stream region. In particular $MSST_M$ predicts relatively large oscillations in the path of the Gulf Stream downstream of the New England seamount chain that are not evident in the drifter velocities or the zero contour of sea level skewness. We speculate that the oscillations in $MSST_M$ are due to deficiencies in the climatology to which the ocean model was spectrally nudged, i.e., the problems are associated with $MSST_M$. We speculate that the climatology, which is based on hydrographic observations spread over most of the last century, may have aliased the variability in the hydrography in this energetic region. Work is presently underway to test this idea and also to develop a new climatology based on hydrographic data for just the satellite era.

[43] It is important to note that $MSST_{G1}$ also contains some oceanographically unrealistic features including high wave number variability south of Iceland and spikes in the vicinity of Madeira, the Canary Islands and Cape Verde. The comparison of MSSTs, as carried out for example in the present study, is clearly beneficial to both the ocean and geodetic communities in terms of mapping surface currents and also checking and refining the geoid.

[44] Given the realism of $MSST_{G1}$, an important question is how best to assimilate such data into forecast models of ocean mesoscale variability. Our experience with eddy-permitting models of the North Atlantic is that the MSST in the Gulf Stream region is very sensitive to the parameterization of mixing and the structure of deep western boundary currents. The approach that we are taking is to use the MSST, along with fields of standard deviation and skewness, to optimize parameters (e.g., mixing coefficients) and open boundary conditions in order to bring the model's first three moments of sea level variability into agreement with observations. After this step has been taken, sea level from altimeters and in situ data (e.g., temperature and salinity profiles from Argo floats) will be assimilated using sequential schemes that are tuned to the ocean mesoscale.

Appendix A: Calculation of the Regional Geoid (N)

[45] The overall idea is to first "condense" the Earth's topography on to an infinitesimally thin layer coincident with the geoid, solve a geodetic boundary value problem using the approach of Stokes to find the Helmert geoid, and then correct for the height difference between the Helmert geoid and the true geoid. These steps are evident in the following approximate equation used to calculate the true geoid height with respect to the reference ellipsoid:

$$N = c + N_H + \delta N_{pite}. \tag{A1}$$

[46] The quantity c is the sum of 3 correction terms associated with the Earth's mass, the reference gravity potential and the geocenter with respect to the reference frame. N_H is the height of the Helmert geoid. The last term, δN_{pite}, depends on the mean density and height of the Earth's topography and corrects N_H for errors caused by the condensation; it is called the primary indirect topographic effect.

[47] In this study, the Helmert geoid is calculated from a combination of satellite and terrestrial gravity data,

$$N_H = N_H^S + \frac{R}{4\pi\gamma}\int_\Omega S^W(\psi)\left(\Delta g^{TH} - \Delta g^{SH}\right)d\Omega. \tag{A2}$$

[48] The quantity N_H^S is the Helmert geoid calculated from a satellite-based gravity model. In the present study, N_H^S is specified only for long wavelengths. The quantities R and γ are the mean radius of the Earth and normal gravity on the reference ellipsoid. The region of integration, Ω, is confined to a spherical cap centered on the computation point of interest. The integrand is the weighted product of (1) the weighted degree-banded Stokes kernel function, $S^W(\psi)$, that varies only with spherical angular distance ψ from the center of the cap and (2) the difference between observed terrestrial gravity anomalies on the Helmert geoid (Δg^{TH}) and satellite gravity anomalies (Δg^{SH}). The weighted degree banded Stokes kernel function allows a proper combination of the GRACE and terrestrial gravity data.

[49] The above method has been used to calculate the geoid for the region 7°N to 67°N, 99°W to 20°E. The Helmertized GGM02C model of *Tapley et al.* [2005] was used to calculate N_H^S and Δg^{SH} using spherical harmonics ranging from spherical harmonic degree 2 to 60. A terrestrial gravity data set was used to calculate Δg^{TH}. The data set includes land observations from Canada and the United States, shipboard observations from the east coast of Canada (extending seaward about 500 km) (see Figure 1), and airborne data from Greenland. The altimetry-derived gravity data cover the rest of the region. The adopted weight scheme allows the geoid to be determined solely from GRACE below spherical harmonic degree 60 (660 km wavelength), from a weighted blend of the GRACE, terrestrial and altimeter-derived gravity data between spherical harmonic degrees 60 to 90, and solely from the terrestrial and altimeter-derived data above degree 90. This scheme makes the geoid solution less affected by the stripping error in the GRACE model around spherical degree 90 and full use of the terrestrial gravity data where available. The region of the Stokes integration was a spherical cap of 6 arc degrees (a spherical angle distance of about 660 km). The far zone contribution outside of the spherical cap is evaluated from GGM02C with an accuracy better than 2 cm.

[50] The regional geoid was calculated using (A1) and (A2) on a grid with a spacing of 2 arc minutes (1/30°) in

both latitude and longitude. The actual intrinsic spatial resolution varies from place to place, dependent on the spatial density of terrestrial data (which is about one data point per 10 km on average). The use of the finer grid is the most efficient way of using the terrestrial gravity data in terms of spectral content, i.e., the MSST can be determined as finely as possible wherever proper terrestrial data are available. However, for areas for which only satellite gravity data are available, the resulting MSST does not contain independent components above spherical harmonic degree 90. Another advantage of using the combined geoid is the avoidance of filtering or spherical harmonic smoothing. A few authors [*Jayne*, 2006; *Vianna et al.*, 2007; *Vossepoel*, 2007] have discussed and analyzed the filtering error in detail.

[51] There are 3 main types of random error that affect the accuracy of the geoid, N, that is computed using this approach. First there is the random error in N_H^S which can be estimated from the standard errors of the coefficients defining the gravity model, GGM02C. The result is a standard deviation of about 2 cm. The second error is due to errors in the terrestrial gravity anomalies, Δg^{TH}. Within about 500 km from shore the standard error of Δg^{TH} is due to errors in the land and shipboard gravity measurements and these have been estimated to produce a standard error of less than about 2 cm. The post glacial rebound effect on the terrestrial data are not significant and can be neglected. Outside of this region the standard error of Δg^{TH} has been assigned a constant value of 15 mGal, representing a worst case scenario based on comparisons between them and shipboard data. This corresponds to a geoid height error of less than about 5 cm. The third type of error is associated with the far zone contribution (i.e., outside the spherical cap, which is more than 6 degrees from the computation point); on the basis of the standard errors of the GGM02C coefficients it leads to a spatially uniform, standard error of about 1.6 cm. (Note that the correlation between the GGM02C coefficients, although significant, was ignored in the above analysis and so the resulting error estimates should be considered as only approximate (M. Cheng, personal communication, 2005)).

[52] In summary, within about 500 km of the east coast of Canada, the standard error of the regional geoid due to the 3 random errors is estimated to be $\sqrt{2^2 + 2^2 + 1.6^2} = 3.2$ cm. Outside of this coastal region the standard error is estimated to be $\sqrt{2^2 + 5^2 + 1.6^2} = 5.6$ cm.

[53] When the mean sea surface height (MSSH) measured by satellite altimetry is inverted to estimate the gravity anomaly, the mean sea surface topography (MSST) must be removed from the MSSH. Because the MSST is unknown, an approximate MSST is used, resulting in errors in the derived gravity anomaly. In the case of the GSFC00 gravity grid, an MSST model complete to spherical harmonic degree and order 20 was removed (Y. Wang, personal communication, 2007). Since the GRACE model defines the geoid up to degree and order 60, the use of the surface topography model has no impact on the derived MSST in principle. The leakage caused by the combination method has been studied, and is smaller than 2 cm. For ocean areas without shipboard or airborne gravity data, the MSST_G beyond the resolution of GRACE data (i.e., spherical degree 90) is subject to unknown correlation error because of the use of the altimetry-derived gravity anomaly in the geoid modeling. This correlation error tends to cancel out any MSST components with wavelengths greater than 450 km (corresponding to spherical harmonic degree 90).

Appendix B: Ocean Model

[54] The ocean model used in this study is version 2.0 of the Parallel Ocean Program (POP) [see *Smith et al.*, 1992]. It is a z-coordinate, hydrostatic general ocean circulation model with an implicit free surface. The model grid covers the North Atlantic basin between 7°N and 67°N. It has 23 vertical levels and a horizontal resolution of 1/3° in longitude and 1/3° cos ϕ in latitude (ϕ). The grid boxes are thus approximately square and range in size from 37 km to 14 km from south to north. The model is therefore eddy permitting but not eddy resolving over the whole domain. The vertical mixing is parameterized by the KPP scheme of *Large et al.* [1994] and the horizontal mixing is biharmonic with a tracer mixing coefficient of -5×10^{18} cm^4 s^{-1} and a momentum coefficient of -2 $\times$ 10^{19} cm^4 s^{-1}. Temperature and salinity are relaxed to the seasonal climatology of Yashayaev within "sponge layers" with a meridional extension of 3 degrees from the closed northern and southern boundaries. The relaxation coefficient is 1/5 d^{-1} at the boundaries of the model domain and it decreases smoothly to 0 as the interior is approached.

[55] The model was first spun up for 30 years, driven by climatological monthly mean surface fluxes calculated from the COADS data set and spectrally nudged toward the observed seasonal temperature and salinity climatology of Yashayaev. The model was then run for the period 1991 to 1999 using (1) surface fluxes computed from the model's sea surface temperature and atmospheric daily mean parameters from the NCEP reanalysis [*Kalnay et al.*, 1996] and (2) surface water fluxes calculated from the monthly mean precipitation data of *Xie and Arkin* [1997].

[56] It is accepted that ocean models of the type used in this study generally drift such that the model's temperature and salinity fields diverge from the observational estimates. We overcame this problem by nudging the model's temperature and salinity fields at all locations toward the seasonal climatology of Yashayaev. To avoid overconstraining the model, we used the spectral nudging technique of *Thompson et al.* [2006] which only nudges the model toward the observed climatology in specified frequency and wave number bands; outside of these bands the model is free to evolve prognostically. Spectral nudging is based on adding to the temperature and salinity forecasts at time t (X_t^f) a term of the form $\lambda\langle X_t^c - X_t^f\rangle$ where X_t^c is the corresponding observed climatological value and $\langle\cdot\rangle$ denotes a filtered quantity that is nonzero only at wavelengths above a specified cutoff and within a frequency band of width κ (in the present case 1/1000 d^{-1}) of the climatological frequencies of $\omega_c = 0$, 1 cycles per year. Note that the time filter used in the determination of spectral nudges has zero phase shift at the climatological frequencies. (For more details on the technique, including the spectral characteristic of the fourth-order Butterworth filter used to spatially smooth the nudges [see *Thompson et al.*, 2006].)

[57] **Acknowledgments.** We thank Igor Yashayaev for providing his seasonal climatology of the North Atlantic and Peter Niiler for providing the drifter velocities. K.R.T. acknowledges support from the GEOIDE research network, the GOAPP research network, and the NSERC Discovery Grant program. D.W. acknowledges support from the DFO COMDA center of expertise and the GOAPP research network.

References

Bingham, R., and K. Haines (2006), Mean dynamic topography: Intercomparisons and errors, *Philos. Trans. R. Soc. Ser. A*, *364*, 903–916.

Ducet, N., and P. Y. Le Traon (2001), A comparison of surface eddy kinetic energy and Reynolds stresses in the Gulf Stream and the Kuroshio Current systems from merged TOPEX/Poseidon and ERS-1/2 altimetric data, *J. Geophys. Res.*, *106*, 16,603–16,662.

Hakkinen, S., and P. Rhines (2007), Shifting surface currents in the northern North Atlantic Ocean, *J. Geophys. Res.*, *114*, C04005, doi:10.1029/2008JC004883.

Heiskanen, W. A., and H. Moritz (1967), *Physical Geodesy*, W.H. Freeman, San Francisco, Calif.

Huang, J., and M. Véronneau (2005), Applications of downward continuation in gravimetric geoid modeling — Case studies in western Canada, *J. Geod.*, *79*, 135–145.

Jayne, S. (2006), Circulation of the North Atlantic Ocean from altimetry and the Gravity Recovery and Climate Experiment geoid, *J. Geophys. Res.*, *111*, C03005, doi:10.1029/2005JC003128.

Kalnay, E., et al. (1996), The NCEP/NCAR 40-year Reanalysis Project, *Bull. Am. Meteorol. Soc.*, *77*, 437–471.

Large, W., J. McWilliams, and S. Doney (1994), Oceanic vertical mixing: A review and a model with a nonlocal boundary layer parameterization, *Rev. Geophys.*, *32*, 363–403.

Lazier, J., and D. Wright (1993), Annual velocity variations in the Labrador Current, *J. Phys. Oceanogr.*, *23*, 659–678.

Le Traon, P.-Y. (2002), Satellite oceanography for ocean forecasting, in *Ocean Forecasting*, edited by N. Pinardi and J. D. Woods, pp. 19–36, Springer, New York.

Mann, C. (1967), The termination of the Gulf Stream and the beginning of the North Atlantic Current, *Deep Sea Res. Oceanogr. Abstr.*, *14*, 337–359.

Niiler, P. (2001), The world ocean surface circulation, in *Ocean Circulation and Climate — Observing and Modelling the Global Ocean*, edited by J. Church, G. Siedler, and J. Gould, pp. 193–204, Academic, London.

Niiler, P., and J. Paduan (1995), Wind-driven motions in the northeast Pacific as measured by Lagrangian drifters, *J. Phys. Oceanogr.*, *25*, 2819–2830.

Reigber, C., R. Schmidt, F. Flechtner, R. Konig, U. Meyer, K. Neumayer, P. Schwintzer, and S. Zhu (2005), An Earth gravity field model complete to degree and order 150 from GRACE: EIGENGRACE02S, *J. Geodyn.*, *39*, 1–10.

Reverdin, G., P. Niiler, and H. Valdimarsson (2003), North Atlantic ocean surface currents, *J. Geophys. Res.*, *108*(C1), 3002, doi:10.1029/2001JC001020.

Rio, M.-H., and F. Hernandez (2004), A mean dynamic topography computed for the world ocean from satellite altimetry, in situ measurements and a geoid model, *J. Geophys. Res.*, *109*, C12032, doi:10.1029/2003JC002226.

Sarmiento, J., and K. Bryan (1982), An ocean transport model for the North Atlantic, *J. Geophys. Res.*, *87*, 394–408.

Smith, R., J. Dukowicz, and R. Malone (1992), Parallel ocean general circulation modeling, *Physica D*, *60*, 38–61.

Tapley, B., D. Chambers, S. Bettadpur, and J. Ries (2003), Large scale ocean circulation from the GRACE GGM01 geoid, *Geophys. Res. Lett.*, *30*(22), 2163, doi:10.1029/2003GL018622.

Tapley, B., S. Bettadpur, M. Watkins, and C. Reigber (2004), The gravity recovery and climate experiment: Mission overview and early results, *Geophys. Res. Lett.*, *31*, L09607, doi:10.1029/2004GL019920.

Tapley, B., et al. (2005), GGM02 — An improved Earth gravity field model from GRACE, *J. Geod.*, *79*, 467–478.

Thompson, K., and E. Demirov (2006), Skewness of sea level variability of the world's oceans, *J. Geophys. Res.*, *111*, C05005, doi:10.1029/2004JC002839.

Thompson, K., D. Wright, Y. Lu, and E. Demirov (2006), A simple method for reducing seasonal bias and drift in eddy resolving ocean models, *Ocean Modell.*, *13*, 109–125.

Vanicek, P., and Z. Martinec (1994), The Stokes-Helmert scheme for the evaluation of a precise geoid, *Manuscr. Geoid.*, *19*, 119–128.

Vianna, M., V. Menezes, and D. Chambers (2007), A high resolution satellite-only GRACE-based mean dynamic topography of the South Atlantic Ocean, *Geophys. Res. Lett.*, *34*, L24604, doi:10.1029/2007GL031912.

Vossepoel, F. (2007), Uncertainties in the mean dynamic topography before the launch of the Gravity Field and Steady-State Ocean Circulation Explorer (GOCE), *J. Geophys. Res.*, *112*, C05010, doi:10.1029/2006JC003891.

Wang, Y. (2001), GSFC00 mean sea surface, gravity anomaly, and vertical gravity gradient from satellite altimeter data, *J. Geophys. Res.*, *106*, 31,167–31,174.

Xie, P., and P. A. Arkin (1997), Global precipitation: A 17-year monthly analysis based on gauge observations, satellite estimates, and numerical model outputs, *Bull. Am. Meteorol. Soc.*, *78*, 2539–2558.

J. Huang and M. Véronneau, Geodetic Survey Division, CCRS, Natural Resources Canada, 615 Booth Street, Ottawa, ON K1A 0E9, Canada.

Y. Lu, Environment Canada, 45 Alderney Drive, Dartmouth, NS B2Y 2N6, Canada.

K. R. Thompson, Department of Oceanography, Dalhousie University, Halifax, NS B3H 4J1, Canada. (keith.thompson@dal.ca)

D. G. Wright, Department of Fisheries and Oceans, Bedford Institute of Oceanography, Dartmouth, NS B2Y 4A2, Canada.